Vol. 39 (2008) *ACTA PHYSICA POLONICA B* No 10

DARK MATTER DETECTION WITH CRYOGENIC NOBLE LIQUIDS*

Elena Aprile

Physics Department and Columbia Astrophysics Laboratory
Columbia University, New York, NY 10027, USA
age@astro.columbia.edu

(Received August 29, 2008)

Observations on all fronts strongly support the view of a universe composed of $> 96\%$ invisible matter and energy. The invisible matter is non-baryonic, cold and likely in the form of new particles generically referred to as Weakly Interacting Massive Particles (WIMPs), relics from the early universe. One way to detect WIMPs is to measure the nuclear recoils produced in their rare elastic collisions with ordinary matter. The predicted interaction rate ranges from the best sensitivity of existing experiments of ~ 1 evts/kg/yr to ~ 1 evts/1000 kg/yr. Efforts are underway worldwide to realize sensitive direct detection experiments, with large target mass and improved background rejection capabilities. In this talk I will review experiments headed in this direction with the use of cryogenic noble liquids, focusing on those experiments which use the common technique of a dual-phase (liquid/gas) time projection chamber to measure simultaneously the ionization and the scintillation signals produced by radiation in a large volume of liquid xenon or liquid argon. The four experiments I will review are XENON, ZEPLIN, WARP and ArDM.

PACS numbers: 95.35.+d, 14.80.Ly, 29.40.Mc, 95.55.Vj

1. Introduction

The nature of dark matter and dark energy, which compose >96% of the universe (see [1], and references therein), is one of the most fundamental questions in physics. The leading candidate for the invisible "dark matter" is relics from the early universe known as Weakly Interacting Massive Particles (WIMPs). Such particles are also predicted by extensions of the standard model of particle physics, such as Supersymmetry (SUSY) [2]. If WIMPs

* Presented at the XXXVI International Meeting on Fundamental Physics, Baeza (Jaén), Spain, February 4–8, 2008.

exist, they are also the dominant mass in our own Milky Way, and, though they only very rarely interact with conventional matter, should nonetheless be detectable by sufficiently sensitive detectors on Earth.

In direct detection, one measures the energy, typically a few tens of keV [3], of the nuclear recoil which results from a WIMP-nucleon elastic scattering. A variety of target nuclei and detectors are used in direct detection experiments worldwide.

For a recent review of the field we refer to the report by the DUSEL S1 Dark Matter Working Group ([4], and references therein). Covering the bulk of the SUSY parameter space for WIMPs will require a sizable increase in sensitivity from the current best experimental limits [5,6]. An increase in detector mass and exposure, in addition to a reduction in and/or improved rejection of radioactive and cosmogenic backgrounds is necessary.

The predicted event rates for a WIMP mass of 100 GeV/c^2 and a spin-independent WIMP-nucleon cross-section of 10^{-44} cm^2 are shown in Fig. 1 for Ge, Xe and Ar targets. The fast fall of the event rate with increasing recoil energy demands a very low energy threshold, around 10 keV. At this energy, the event rate for a Xe target is about 30% higher than for a Ge target, due to the Xe larger atomic number. Cryogenic solid state detectors, based on Ge and Si crystals, have for a long time dominated the field of dark matter direct detection, showing the best background discrimination and reporting stringent spin-independent WIMP-nucleon cross-section (4.6×10^{-44} cm^2 at a WIMP mass of 60 GeV/c^2 [6]).

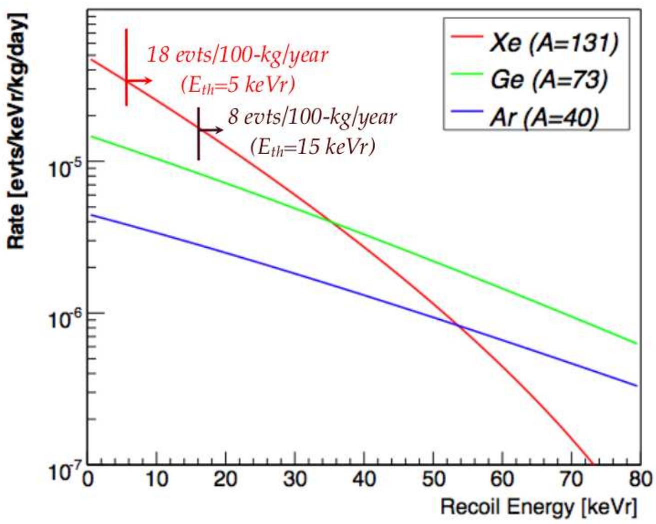

Fig. 1. Event rates for a 100 GeV/c^2 WIMP with spin-independent WIMP-nucleon cross-section of 10^{-44} cm^2 for different target materials.

In recent years, however, the application of cryogenic noble liquids in dark matter searches, has gained new momentum due to their promise for large target mass detectors with possibly as powerful background discrimination as cryogenic crystals. LXe and LAr are especially attractive as they are known to be good scintillators and ionizers, as established in many works. The scintillation mechanism in these liquids is well known [7]. Both excitation and electron–ion pairs recombination produce excited dimmers, which lead to scintillation light ($\mathrm{Xe}_2^* \rightarrow 2\mathrm{Xe}+h\nu$ in the case of Xe). In pure liquids, the light pulse has two decay components due to de-excitation of singlet and triplet states of the excited dimers. These components have decay times which depend strongly on the ionization density of the particle. For alpha-particles in LXe the shorter decay time produced from the de-excitation of singlet states and the longer one from the de-excitation of triplet states, are 4.2 and 22 ns. However, the scintillation for relativistic electrons has only one decay component whose effective decay time is 45 ns. This is due to the slow recombination between electrons and ions produced by relativistic electrons, since this component disappears if some electric field is applied. The decay shape of scintillation light from energetic electrons in LXe, under an electric field of 4 kV/cm, has the usual two decay components, with the short one being 2.2 ns and the longer one being 27 ns. In LAr, these components have decay times which are much more separated, allowing for an easier pulse shape discrimination (PSD) of the scintillation signal as background rejection tool. The ionization electrons which escape recombination can be collected with an applied electric field. The recombination process strongly depends on the ionization density of the radiation and its track structure, so that the ratio of ionization to scintillation in noble liquids is different for electron recoils from gamma and beta background and for nuclear recoils from WIMPs and neutron background. The simultaneous detection of charge and light therefore provides background discrimination in LXe and LAr, in a similar way as the simultaneous detection of charge and phonon signals provides discrimination in cryogenic Ge and Si. In addition to being available in large quantities for cost effective large volume detectors, another advantage of LAr and LXe over cryogenic solid state detectors is their high boiling point, 87 K and 165 K respectively, which require much less complex cryogenic systems.

I will briefly review four experimental efforts for dark matter direct detection all based on the simultaneous measurement of charge and light in either Xe or Ar dual-phase time projection chambers (TPCs). In these detectors, the ionization electrons which survive recombination and trapping by impurities are drifted towards the liquid surface where they are extracted into the gas and detected either with a charge readout or a photon readout, in the case of induced proportional scintillation in the gas. The energy threshold, the x–y spatial resolution, the background rejection power, the radio-purity of the materials, the gamma and neutron shielding, the underground environment and depth, all contribute to the different sensitivity projected for these experiments.

2. The XENON Dark Matter experiment

The goal of the XENON Dark Matter phased program is to realize a very sensitive, low background, dual-phase TPC containing 1000 kg of Xe as fiducial target, to search for both spin-independent and spin-dependent coupling of WIMPs with matter. With an energy threshold of 5 keV, nuclear recoil equivalent, and a total background event rate lower than 10^{-4} evts/kg/keV/yr before any rejection, the sensitivity goal of XENON1T is at the 10^{-47} cm^2 level, or about almost four orders of magnitude lower than the current best sensitivity.

In the XENON Dark Matter experiment, the simultaneous detection of ionization and scintillation in a liquid xenon 3D position sensitive time projection chamber is used to identify nuclear recoils, produced by WIMPs (and neutrons), from electron recoils produced by gamma and beta background, with a rejection power better than 99.5%.

The XENON10 detector was deployed at the Gran Sasso Underground Laboratory (LNGS) [8] in spring of 2006 and the first results from a WIMP search were obtained in spring of 2007, making XENON10 the most sensitive dark matter experiment worldwide. Fig. 2 shows the 90% C.L. upper limit on the spin-independent cross-section of a WIMP with nucleons of 8.8×10^{-44} cm^2 for a WIMP mass of 100 GeV/c^2 [5]. The result is based on 58.6 live days, acquired between October 2006 and February 2007. The same data were also analyzed for spin dependent coupling of WIMPs to matter [9]. The result for pure neutron couplings are the world's most stringent to date, reaching a minimum cross-section of $5{\times}10^{-39}$ cm^2 at a WIMP mass of 30 GeV/c^2 (Fig. 3). We also exclude a heavy Majorana neutrino with a mass in the range of $\sim$ 10 GeV/c^2–2 TeV/c^2 (Fig. 4) as a dark matter candidate under standard assumption for its density and distribution in the galactic halo.

The excellent performance of this first generation TPC has enabled the LXe technology to be at the forefront of dark matter direct detection and the renewed XENON Collaboration is currently pursuing an aggressive second phase of the program with the XENON100 experiment.

At the time of this writing, XENON100 had just began operation underground, in the modified shield previously used for XENON10. Following several months of calibration runs, the first WIMP search run will start by the end of 2008. We expect to achieve the XENON100 sensitivity goal of $\sim 2 \times 10^{-45}$ cm^2 within 2009 (see Fig. 5).

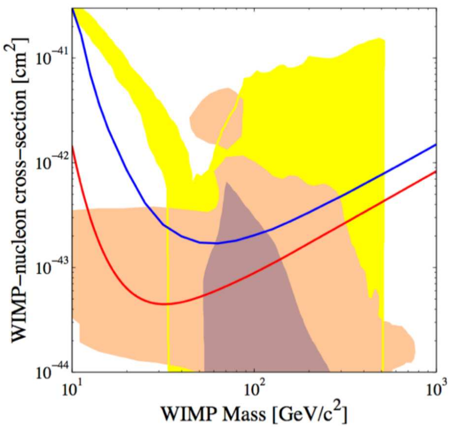

Fig. 2. Spin-independent WIMP-nucleon cross-section upper limits (90% C.L.) *versus* WIMP mass. Shown curves are for the previously best published limit (upper, blue) and the current work (lower, red). The shaded area is for parameters in the MSSM models (light-grey, yellow), the Constrained MSSM models (grey, marron) and CMSSM with the recent improved Standard Model prediction for the branching ratio of $\bar{B} \Rightarrow X_s\gamma$ (dark-grey, brown).

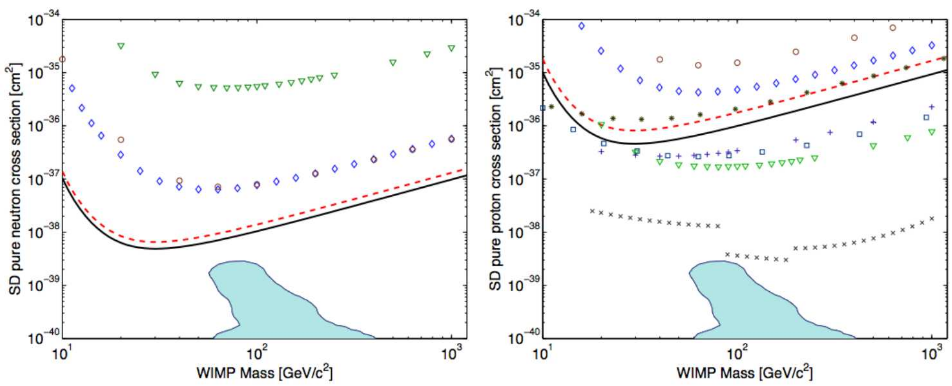

Fig. 3. Combined 90% C.L. exclusion Limits for ^{129}Xe and ^{131}Xe for pure neutron (left) and pure proton (right) couplings (solid curves). The dashed curves show the combined Xe limits using the alternate form factor. Also shown are the results from the CDMS experiment (diamonds), ZEPLIN-II (circles), KIMS (triangles), NAIAD (squares), PICASSO (stars), COUPP (pluses) and SuperK (crosses). The theoretical regions (constrained minimal supersymmetric model) are also shown.

The XENON100 detector is a dual phase TPC, in which ionization electrons produced by an event in the liquid xenon are efficiently extracted from the liquid to the gas, with subsequent amplification via proportional

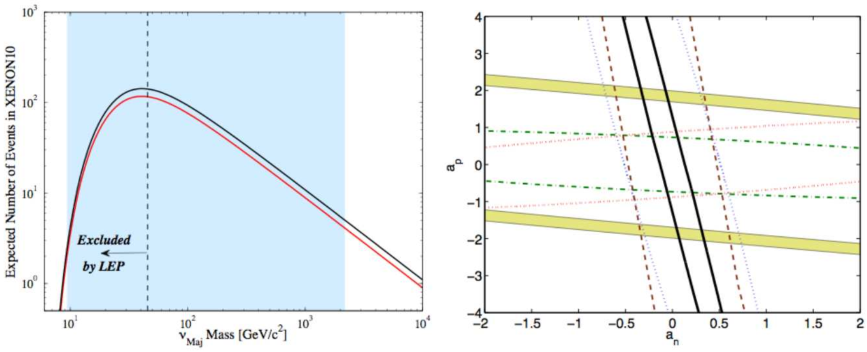

Fig. 4. Left: Predicted number of events in XENON10 for a heavy Majorana neutrino with standard weak interaction as a function of the neutrino mass, using the main (upper, black) and alternate (lower, red) form factors. The light shaded area shows the excluded mass region at 90% C.L. Right: Regions allowed at the 90% C.L. in a_n–a_p parameter space for a WIMP mass of 50 GeV/c^2. The combined limit from ^{129}Xe and ^{131}Xe is shown as a dark solid curve (using the main form factor). The exteriors of the corresponding ellipses are excluded, the common space inside the ellipses being allowed by the data. We also show the results obtained by KIMS (dot-dashed), COUPP (horizontal ellipses) and CDMS (dotted), ZEPLIN-II (dashed) and the DAMA evidence region(vertical ellipses).

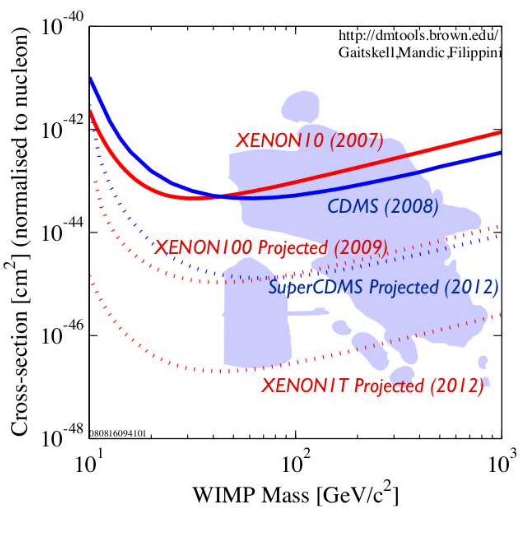

Fig. 5. WIMP-nucleon cross-section upper limit (90% C.L.) from direct dark matter search experiments. The projected upper limits are shown as dashed lines.

scintillation. The ratio of the amplitude of the charge and light signals, being quite distinct for nuclear and electron recoils, provides the basis for event-by-event discrimination in the XENON concept. A schematic of the XENON100 TPC is shown in Fig. 6. The XENON100 detector consists of an inner target surrounded by an active LXe veto. Both target and veto are contained in a single double-walled vacuum cryostat made of low activity stainless steel (SS). The total mass of Xe required to fill the detector is 170 kg, of which approximately 70 are in the fiducial volume (target). The light readout is based on the same type of 1 inch square photomultiplier tubes (PMTs) as used in XENON10 (Hamamatsu R8520-06-AL), but with selected low radioactivity materials. Seventy of the 250 tubes used for the target and veto readout are of the higher QE type. The target will be again seen by a top and bottom array of PMTs, as in XENON10. An important background rejection feature of the XENON100 detector is the ability to localize events in 3D with a spatial resolution a few mm in x–y and <1 mm in z.

The target is enclosed by a teflon structure, made with interlocking panels. Teflon is used as an effective UV light reflector and as an electrical insulator. The TPC is equipped with four wire meshes, two in the liquid and two in the gas. The bottom mesh serves as cathode and the next one, positioned just below the liquid level, together with a series of field shaping rings, form the 30 cm drift region. The top two meshes, together with the one below the liquid level, serve to define the gas proportional scintillation region. The wire meshes and top PMT array are mounted in an SS cylinder closed on top, but open at the bottom. The cylinder works like a "diving bell", keeping the liquid level at a precise height. A positive pressure in the bell is provided by the gas returning from the continuous recirculation system. The "diving bell" system was developed and used to control the liquid level in the XENON10 detector.

A Pulse Tube Refrigerator (PTR) with 170 W cooling power will be used to liquefy and keep the liquid temperature. As demonstrated with XENON10, the PTR provides excellent long time stability of operation, with temperature deviations not exceeding 0.1°C and pressure changes less than 1%. The key difference is that the cryogenic system which was previously mounted on top of the XENON10 cryostat, inside the Pb/Poly shield enclosure, is now moved outside the shield, to minimize background.

An un-vetoed event in the XENON100 TPC will be of interest if it features only two pulses: one from the direct scintillation light in the liquid (S1, with a characteristic width >100 ns) and one from the ionization charge, amplified via scintillation in the gas (S2, with characteristic a width of a few μs). The two pulses occur within the maximum drift time of 150 μs, for a saturated drift velocity of 2 mm/μs in LXe.

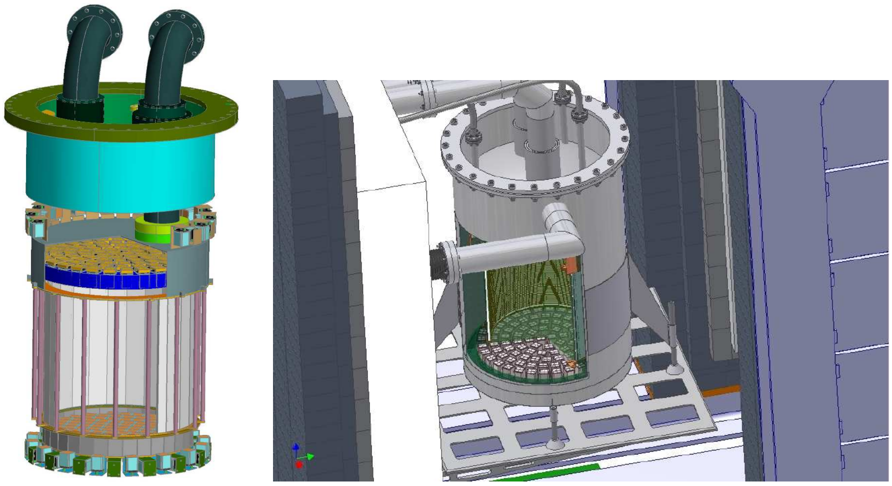

Fig. 6. Schematic of the XENON100 TPC (left) and the cryostat inside the shield (right).

The greatest challenge for the readout electronics is the large dynamic range required: the system must be able to handle signals ranging from single photoelectrons (scintillation signals in the keV range) up to large S2 pulses from gamma ionization signals (up to thousands of photoelectrons). Moreover, the time difference between S1 and S2 pulses must be measured with sub-μs resolution in a 300 μs range, to provide 3D position reconstruction throughout the drift volume (we require twice the maximum drift time, to enable triggering either on the S1 or S2 pulse). We have adopted a DAQ design based on CAEN 1724 Flash ADCs, with a sampling rate of 100 MHz. To reduce the large data rate, zero-suppression is implemented with the FPGA (field programmable gate array) available on each board.

High purity liquid xenon is an essential requirement for a TPC like XENON100, with a drift gap of 30 cm. The purity must be preserved at all time during the detector operation in order to ensure stable performance. With XENON10 we have fulfilled this requirement by continuous gas circulation through a high temperature getter, reaching an electron lifetime of (1.8 ± 0.4) ms. While more challenging, we expect to achieve similar purity level in XENON100. Similarly demanding, is the requirement for very low level contamination of radioactive ^{85}Kr in Xe. By using a dedicated cryogenic distillation column, we will reduce the ^{85}Kr concentration well below the 50 ppt (part per trillion) required by the XENON100 sensitivity goal.

The commissioning of the XENON100 experiment is well underway at LNGS. We have started to calibrate the new TPC and expect to be ready for science data taking by the end of 2008. This new phase in the XENON Dark

Matter Program promises to yield a major advancement in the search for WIMP, with an order of magnitude sensitivity improvement over the best limit reported to-date for spin-independent interactions. XENON100 will also be able to advance the search for spin-dependent WIMP interactions with matter. Finally, XENON100 starts to be competitive also for a dedicated search of an annual modulation signature of WIMPs, with a sizeable target mass, similar energy threshold and lower background than that of inorganic scintillator-based experiments. Within the phase XENON program, the next step is the realization of the XENON1T TPC, to be operational by 2013 with the projected sensitivity shown in Fig. 5. We have started a design study for the tonne scale experiment, with which we will probe the lowest spin independent WIMP-Nucleon cross-section predicted by SUSY.

3. The ZEPLIN experiment

The ZEPLIN II and ZEPLIN III detectors are also dual-phase (liquid/gas) xenon TPCs where background discrimination is accomplished by means of measuring both the VUV scintillation photons and the ionization produced by incident particle interactions. The detectors were built and developed by the ZEPLIN collaboration and are operating at the Boulby Underground Laboratory in the UK at a depth of 2805 m w.e.

A schematic of the ZEPLIN II detector is shown in Fig. 7. The target vessel is made of copper and is surrounded by a stainless steel vacuum vessel. The active volume is defined by a thick PTFE tapered annulus of top and bottom inner radii of 16.2 and 14.2 cm, respectively, for a target mass of 31 kg of liquid xenon. This structure acts both as a VUV scintillation light reflector and as a support for the field shaping rings of the drift volume. A cathode mesh at the bottom and another grid below the liquid surface along with the field shaping rings serve to maintain a 1 kV/cm electric field throughout the volume. To extract the drifted electrons from the liquid and to provide the electroluminescence region in the gas phase, a third grid is placed above the liquid surface. The strong electric field of 8.4 kV/cm in the gas can extract electrons from the liquid with an efficiency of 90%. The target volume is viewed from above by an hexagonal arrangement of 7 quartz-window 13 cm diameter ETL low background D742QKFLB photomultipliers. The phomultiplier signals are digitized using an Acqiris DC265 8 bit 500 Msamples/s with 150 MHz bandwith. The data acquisition system is designed to trigger on the secondary electroluminescence signal for low energy events with a trigger condition of fivefold coincidences above a threshold of 0.4 photoelectron. The digitizers acquire data 100 μs before and after the trigger (maximum drift time is 73 μs) to allow a "loop-back" for higher energy events that triggered on the primary scintillation signal.

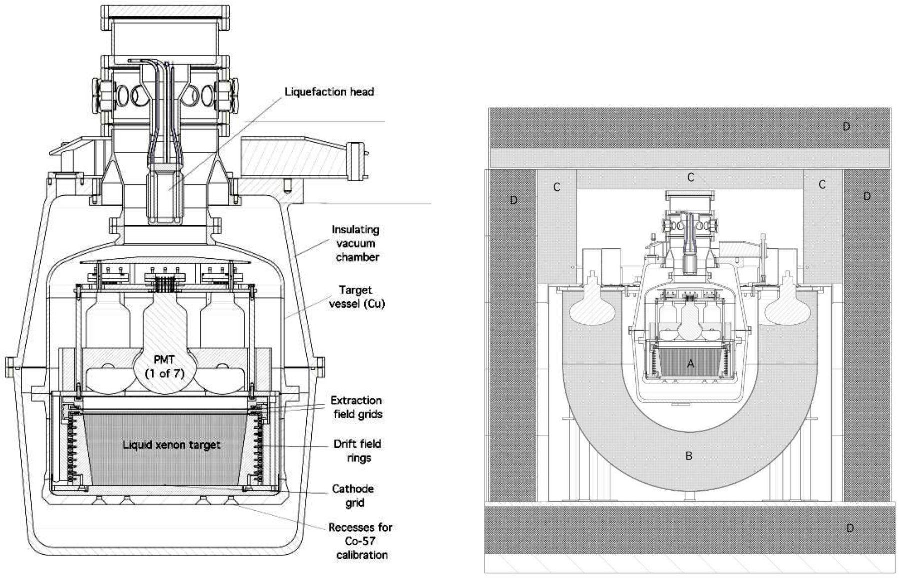

Fig. 7. Schematic of the ZEPLIN II detector (left). The ZEPLIN II detector (A) within its γ (25 cm Pb (D)) and neutron shielding (30 cm Gd-loaded polypropylene (C) and 1 tonne liquid scintillator active veto (B)) (right).

The results from the first underground science run of the ZEPLIN II detector are detailed in [10]. The run had a live time of 31.2 days and a total exposure of 225 kg $\times$ days. A total of 29 events were observed in a 5–20 keV$_{ee}$ window with 50% nuclear recoil acceptance whereas 28.6 ± 4.3 were expected from γ-ray and radon progeny background events. Using the Feldman–Cousins approach, this gives a 90% C.L. upper limit of 10.4 nuclear recoils, corresponding to a WIMP-nucleon spin-independent cross-section of 6.6×10^{-7} pb at a WIMP mass of 65 GeV (Fig. 8 (left)). The results were also converted into limits on WIMP-proton and WIMP-neutron spin-dependent cross-sections [11] (Fig. 8 (right)).

The ZEPLIN III detector was designed to operate at a much higher field than ZEPLIN II and achieve a lower energy threshold [12]. This is accomplished by immersing its photodetectors in the liquid phase and by using a flat planar geometry (Fig. 9). The cylindrical target volume of 19.3 cm radius and 3.5 cm depth is viewed from below by an array of 31 2" ETL D730/9829Q photomultipliers. The drift field and the electroluminescence region are defined by means of a cathode, placed above the PMTs, and a solid 8 mm copper plate ("anode mirror"), 5 mm above the liquid level. In the maximum voltage configuration the cathode will be held at -35 kV and

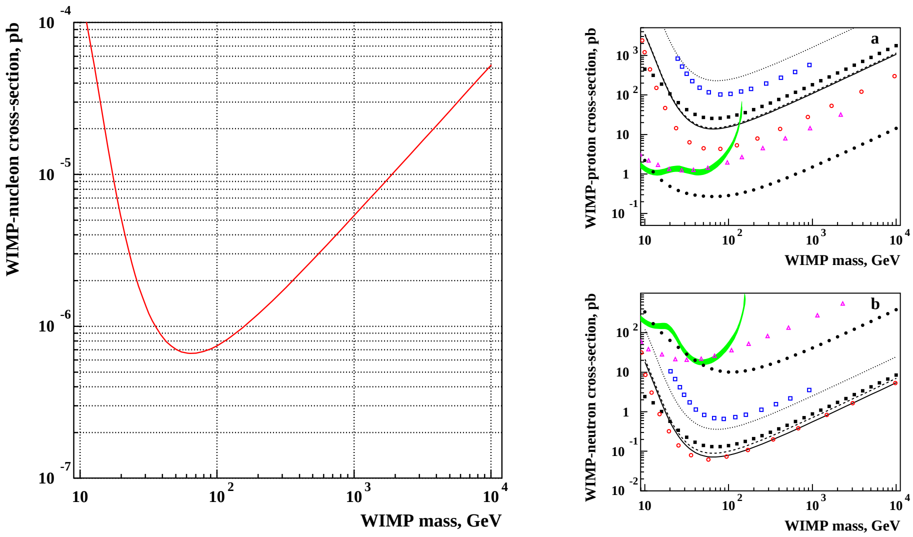

Fig. 8. ZEPLIN II 90% C.L. upper limit on the cross-section of WIMP-nucleon spin-independent interactions (left). 90% C.L. upper limits on the WIMP-proton (right, up) and WIMP-neutron (right, down) spin-dependent cross-sections (solid curves). Also are shown the results from: NAIAD (filled circles), ZEPLIN I (filled squares), CDMS (circles), EDELWEISS (squares) and PICASSO (triangles).

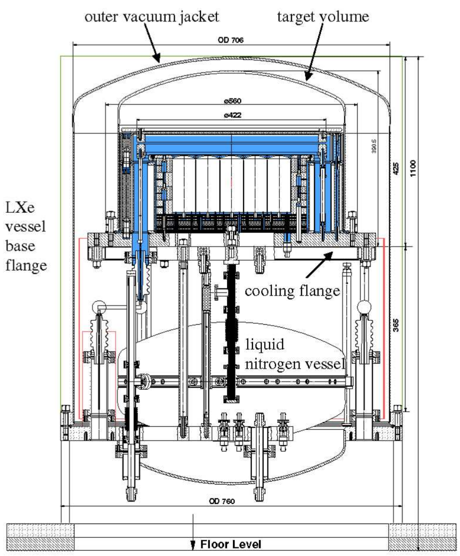

Fig. 9. ZEPLIN III detector.

the anode plate at +5 kV. At these operating voltages the field in the liquid is 8.9 kV/cm and provides a 100% electron extraction efficiency to the gas phase. The pattern of the proportional signals on the PMTs can provide 2D spatial resolution <1 cm while the time interval between the primary and secondary signals can provide a z resolution at the $\sim 50\ \mu$m level. The bulk of the detector parts are made of OFHC copper. Cooling is achieved using liquid nitrogen in a 36 L reservoir located below the target vessel and in contact via two thermal links.

The commissioning of ZEPLIN III was completed in February 2008 and a science run began later that month and ended in May 2008. A final result on the 800 kg $\times$ days of data accumulated is expected shortly and near the predicted sensitivity of $\sim 10^{-7}$ pb [13]. Preparations are on the way for a second science run with low background PMTs and a neutron veto.

4. The WArP experiment

The same principle of a dual-phase TPC, but filled with liquid argon (LAr), is used for the WArP experiment. Background discrimination is accomplished by the simultaneous detection of scintillation photons and ionization and by pulse shape discrimination of the primary scintillation signal, which has a wide separation in rise time between the fast (5 ns) and the slow ($\sim 1.4\ \mu$s) components. In addition, and like in the previous experiments, WArP relies on the power of a 3D position sensitive TPC for additional background rejection. The experiment, located at the Gran Sasso Laboratory, is a phased program with four phases fully approved and funded. For Phase 1, the collaboration built and operated underground a small (2.3 L) dual phase chamber, firstly without and later with a passive neutron shield. In this phase, ordinary argon was used with a high background rate, which has permitted to explore the very high rejection rates in a relatively short time.

The results from this experiment have been published [14] and are shown in Fig. 10.

For Phase 2, the collaboration has focused on reducing ($\sim$1/100) the main background due to the ^{39}Ar natural contamination, by using ^{39}Ar depleted argon. A new 2.3 L chamber made with selected low-radioactive materials is going to be filled with a depleted Ar sample produced by isotopic separation by a commercial manufacturer. Data taking with this new chamber, planned to start in spring of 2008, should improve the sensitivity by about an order of magnitude compared to the previous result. The main effort of the WArP collaboration is however a new 100 L (140 kg) dual phase chamber (Phase 3). The detector is under assembly at LNGS and experimental operation is expected by summer of 2008.

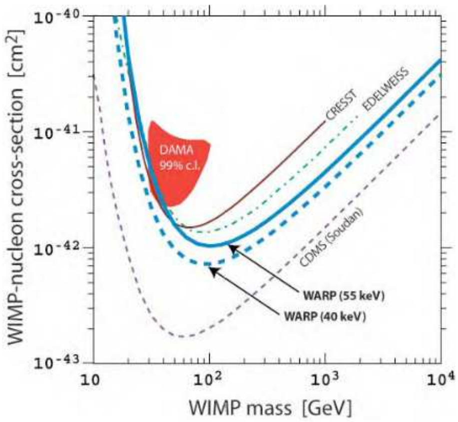

Fig. 10. 90% C.L. spin-independent limits obtained for a total fiducial exposure of 96.5 kgd and a threshold of 55 keV (solid blue curve), and also with a threshold of 40 keV (dashed blue curve).

The WArP 100 L detector layout is schematically shown in Fig. 11 (left). It consists of an external passive shield (a polyethylene 70 cm thick layer as n-shield and a lead 10 cm thick gamma-shield), a 15 ton LAr cryostat (a double wall cryogenic vessel insulated with vacuum and super-insulation and made of stainless steel selected for low radioactive contamination) containing (1) the inner detector (100 L of active LAr target), (2) the active Veto formed by about 8 ton of LAr around the inner detector and (3) externally to the active veto, also immersed in LAr, a 10 cm thick shield of polyethylene.

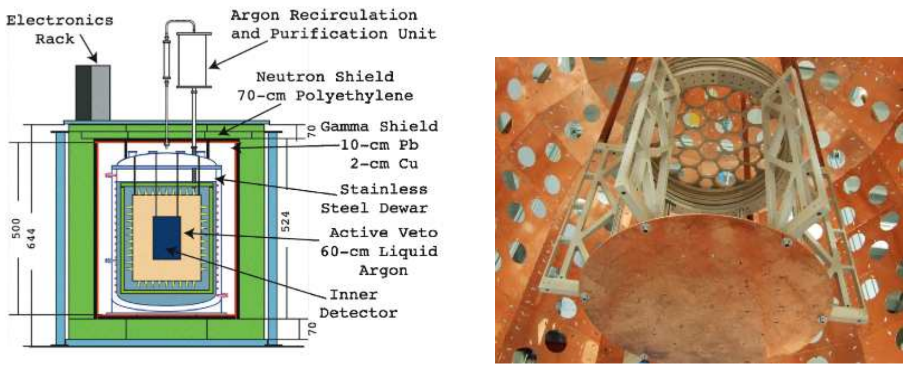

Fig. 11. Warp detector layout.

The inner detector, equipped with field-shaping electrodes for the drift field, grids for extraction of ionization electrons from liquid to the gas phase and proportional light production, and PMTs for the readout of the primary and secondary light signals, is suspended at the center of a LAr volume. This volume works as active shield (veto) against gamma and neutron backgrounds. Minimum thickness of the active LAr shield is 60 cm. It consists of a set of photomultipliers that are held in place by PEEK supports that are connected to a thin copper structure that delimits the external surface of the active shield volume. On the Cu structure are also mounted the basic elements of the waveshifting/reflecting layer (TetraPhenylButadiene waveshifter, deposited on a highly reflective plastic substrate). A total of 436 3" phototubes are installed on the active shield for 10% photocathode coverage of the inner surface and a nominal threshold of 10 keV for argon recoils (10 photoelectrons). The inner detector and the active shield are optically separated (to avoid vetoing of events occurring in the central volume).

The drift field region of the inner detector is delimited by the cathode (a copper disk, 2 mm thick), a set of field shaping rings (copper strips printed on a Kapton foil) and a grid (stainless steel wires stretched on an annular stainless steel frame) placed just below the liquid argon surface. Additional grids, placed in the gas phase, provide the field shaping for extraction from the liquid, acceleration for secondary light production and final collection of ionization electrons. A set of 37 PMTs, placed in the gas phase just above the upper grid, readout the primary and secondary light signals. The gas pocket is enclosed into a copper, vacuum isolated, cup placed upside down. A set of small heating resistors placed just below the liquid surface, together with the heat produced by the PMTs dividers, provide a continuous evaporation of the liquid. The excess gas is evacuated through small holes (1 mm diameter) in the copper cup placed in correspondence of the required level of the liquid to gas interface. This technique ensures both the correct positioning of the liquid level and a continuous recirculation of the LAr in the drift volume. The internal surfaces of the inner detector are also covered with the high reflectivity waveshifting layer to enhance at maximum the scintillation light collection efficiency at the PMT sensitive photo-cathodic area. A foil of copper deposited on Kapton support surrounds the body of the internal detector. This external layer is put to ground and ensures that no residual field is present in the active veto region. Fig. 11 (right) shows the inner detector inside the active veto structure during assembly test at LNGS.

Both the inner detector and the active shield are designed in such a way to reduce as much possible the amount of material request for their assembly and that all materials (mainly copper, PEEK, Kapton and PMTs glass) are selected for a low radioactive contamination. The presence of a wide anticoincidence shield is of primary importance in order to reduce the general background produced externally and internally.

The possibility to fill the inner detector with ^{39}Ar depleted argon obtained from underground reservoirs is presently under consideration.

The sensitivity of WArP (or any argon-based detector) to WIMP dark matter is limited by background from the decay of ^{39}Ar ($E_{\mathrm{max}} = 565$ keV, $t_{1/2} = 260$ yr), a radioactive contaminant of argon in the atmosphere produced by cosmic rays. Its specific activity is 1.01 Bq/kg of argon. The use of ^{39}Ar-depleted argon would eventually allow the construction of multi-ton argon-based WIMP dark matter detectors and the reduction of the main background source intrinsic to the target. Isotopic separation by centrifugation or differential thermal diffusion are established techniques for separation of ^{39}Ar from ^{40}Ar, but on a multi-ton scale could become extremely expensive and require a long production time. Argon from natural gas wells is of potential interest because ^{39}Ar production induced by cosmic rays is strongly suppressed underground. Also, the large quantity of argon stored in underground natural gas reservoirs would be sufficient to provide material for the construction of a multi-ton WIMP detector. A first measurement of ^{39}Ar in argon from underground natural gas reservoirs has been performed during 2007, within the WArP R&D program [15].

Finally, for Phase 4, the sensitive volume of the detector may be extended to 1 ton with minor modifications which will keep the main setup unchanged, including the outer active anticoincidence, depending on the background level attained during Phase 3.

5. The ArDM experiment

The ArDM (Argon Dark Matter) experiment, initiated in 2004, is a direct dark matter search experiment using liquid argon as target medium in a dual-phase TPC. The detector contains 850 kg of liquid argon and provides independent ionization and scintillation light readout. Unlike the previous three experiments, in which the proportional scintillation is detected by PMTs, ArDM uses a charge readout provided by two LEM (Large Electron Multiplier) plates for charge amplification in the gas by means of a high field generated in small (cylindrical shaped) holes.

The ionization electrons are drifted to the liquid-gas interface and are extracted into the gas phase and multiplied by the LEM. The LEM is composed by a 1.5 mm thick plate of isolating material, usually vetronite, which is covered by a copper layer on top and bottom. Holes of about 500 μm in diameter are homogeneously distributed on the LEM, at a distance of 800 μm among them. By placing an electric field between both sides of the plate of ~ 2 kV/mm it is possible to generate an avalanche of electrons and to obtain charge amplification factors $\sim 10^3$–10^4.

The conceptual design of the detector is shown in Fig. 12.

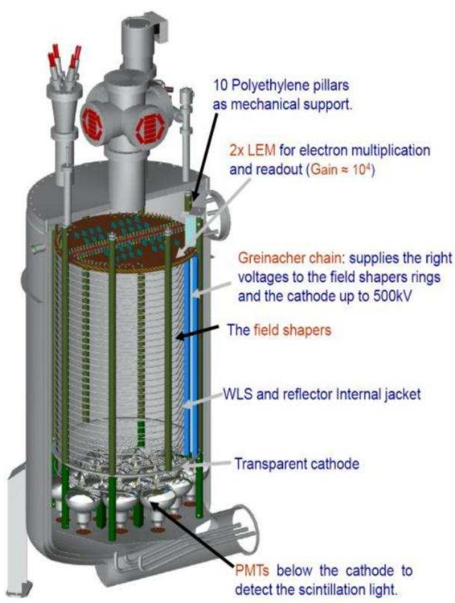

Fig. 12. Schematic of the ArDM detector. Charge and light produced in interactions are readout with a LEM and 14 PMTs. An electric field, uniformized by field shaping rings is used to drift the charge up to the LEM.

The high voltage needed for the electric field over the drift length of 1.2 meters is provided by a Greinacher high-voltage circuit, designed to reach up to 4 kV/cm. A series of electrodes are installed and biased along the full drift path to keep the field uniform at a level of few %. To detect the primary scintillation light an array of 14 PMTs, sensitive to visible light, are used at the bottom of the drift volume, immersed in LAr. Like in WARP, the 128 nm Ar wavelength is shifted into the visible with TPB.

The inside of the field shaping rings is covered with 3M reflecting foils coated with TPB to shift to visible and reflect the scintillation light of liquid argon. Fig. 13 shows pictures of the vessel and the actual detector with the light collection system already mounted.

ArDM expects to be able to reject the dominant background from the internal ^{39}Ar signal using both the simultaneous charge and light, and pulse shape discrimination. The ^{39}Ar isotope is present in natural argon liquefied from the atmosphere, and produces a background rate due to beta decay of approximately 1 kHz in one ton of liquid argon. The ArDM group, like others, is also studying the alternative possibility of using ^{39}Ar-depleted argon extracted from underground natural gas wells. The 1-ton prototype is currently under construction at CERN. It is expected that the experiment

Fig. 13. Left: Inner ArDM detector. In the image the installed PMTs, field shaping rings and the external part of the wavelength shifter sheets can be seen. Right: ArDM vessel. The empty flange on top connects the vessel with the purification and recirculation systems.

will be operated at the Canfranc underground laboratory. With a recoil energy threshold of 30 keV, the sensitivity of the ArDM 1-ton prototype would access the WIMP-nucleon cross-section region of 10^{-42} cm^2. By improving the background rejection power and further limiting the background sources, a two orders of magnitude better sensitivity is projected.

My work on the XENON Dark Matter Project is supported by the National Science Foundation with Award No. PHY-0705337 to the Columbia Astrophysics Laboratory.

REFERENCES

[1] D.N. Spergel *et al.*, *Astrophys. J. Suppl.* **170**, 377 (2007).

[2] A. Bottino, *AIP Conf. Proc.* **751**, 46 (2005).

[3] J.D. Lewin, P.F. Smith, *Astropart. Phys.* **6**, 87 (1996).

[4] D.S. Akerib *et al.*, `astro-ph/0605719v3`.

[5] J. Angle *et al.* [XENON Collaboration], *Phys. Rev. Lett.* **100**, 021303 (2008).

[6] Z. Ahmed *et al.* [CDMS Collaboration], `astro-ph/0802.3530v2`.

[7] A. Hitachi *et al.*, *Phys. Rev.* **B27**, 5259 (1983).

[8] LNGS web page, `http://www.lngs.infn.it`

[9] J. Angle *et al.* [XENON Collaboration], `astro-ph/0805.2939v1`.

[10] G.J. Alner *et al.* [ZEPLIN Collaboration], *Astropart. Phys.* **28**, 287 (2007).

[11] G.J. Alner *et al.* [ZEPLIN Collaboration], *Phys. Lett.* **B653**, 161 (2007).

[12] D.Yu. Akimov *et al.* [ZEPLIN Collaboration], *Astropart. Phys.* **27**, 46 (2007).

[13] H.M. Araujo *et al.* [ZEPLIN Collaboration], *Astropart. Phys.* **26**, 140 (2006).

[14] P. Benetti *et al.* [WArP Collaboration], *Astropart. Phys.* **28**, 495 (2008).

[15] D. Acosta-Kane *et al.* [WArP Collaboration], `astro-ph/0712.0381v1`.